Korean J. Chem. Eng., **24**(2), 299-304 (2007)

Analysis of iron particle growth in aerosol reactor by a discrete-sectional model

Chowdhury G. Moniruzzaman, Hoey G. Park and Kyun Y. Park†

Department of Chemical Engineering, Kongju National University, 182 Shinkwandong, Kongju, Chungnam 314-701, Korea
(*Received 19 July 2006 • accepted 4 October 2006*)

Abstract−The growth of iron particles by thermal decomposition of $Fe(CO)_5$ in a tubular reactor was analyzed by using a one dimensional discrete-sectional model with the coalescence by sintering of neighboring particles incorporated in. A thermal decomposition of $Fe(CO)_5$ vapor to produce iron particles was carried out at reactor temperatures varying from 300 to 1,000 °C, and the effect of reactor temperature on particle size was compared with model prediction. The prediction exhibited good agreement with experimental observation that the primary particle size of iron was the largest at an intermediate temperature of 800 °C. Model prediction was also compared with Giesen et al.'s [1] experimental data on iron particle production from $Fe(CO)_5$. Good agreement was shown in primary particle size, but a considerable deviation was observed in primary particle size distribution. The deviation may be due to an inadequate understanding of the sintering mechanism for the particles within an agglomerate and to the assumption of an ideal plug flow in model reactor in contrast to the non-ideal dispersive flow in actual reactor.

Key words: Iron Particles, Iron Pentacarbonyl, Aerosol Synthesis, Discrete-sectional Model

INTRODUCTION

Iron particles of nanometer size find uses in magnetic recording media, catalysts, and ceramics for medical and pharmaceutical applications. One of the versatile techniques for producing nanosized iron particles is the thermal decomposition of iron pentacarbonyl, $Fe(CO)_5$. Hofmeister et al. [2] used a CO_2 laser as energy source for the decomposition of $Fe(CO)_5$. While, electrically-heated tubular reactors were used in other studies [1,3,4]. These gas-phase reactors where particles of aerosol size are produced are called aerosol reactors. Choi et al. [4] reported that the primary particle size increased with increasing reactor temperature over 400 to 1,100 °C. Park et al. [3] monitored the growth of iron particles along the reactor by investigation of the particles deposited *in situ* on transmission electron microscopy grid, and concluded that the coalescence by sintering between neighboring particles within an agglomerate played an important role in the particle growth. Recently, the influence of the coalescence on the particle size was simulated with a moment model incorporated in Fluent, a computational-fluid-dynamics code [1]. Their model prediction showed good agreement with experimental data, with the activation energy of surface diffusion adjusted to consider the size-dependency of the melting temperature of nanoparticles. The moment model is based on an a priori assumption of log-normal particle size distribution, and its accuracy strongly depends on the validity of the assumption.

In the meantime, sectional and discrete-sectional models were developed to overcome the disadvantage of the moment model. In the sectional model, a continuous size spectrum is approximated by a set of sections, within which all particles are assumed to be of the same size, or a functional form of the size distribution is specified. Xiong and Pratsinis [5] reported a two-dimensional sectional model with particle volume and area as coordinates, enabling prediction of sizes and distributions of agglomerates and primary particles as well, but required enormous computation time to calculate the quadruple integrals for coagulation and sintering coefficients. Simpler one-dimensional sectional models comparable to the two-dimensional model were proposed later by Tsantilis and Pratsinis [6] and Jeong and Choi [7]. The two models differ in the method of approximating the particle size distribution in a section. In the model of Tsantilis and Pratsinis, a representative size was assumed for all the particles in a section, while in the model of Jeong and Choi, the size distribution was assumed to be constant at the mean value determined so that the number of particles in the section can be conserved. The model by Cheong and Choi employs two sets of differential equations: one for the volume and the other for the surface area. By solving the equations simultaneously, the volume and the surface area of each section were obtained, from which average primary-particle size in the section was determined.

The discrete-sectional model is a modification of the sectional

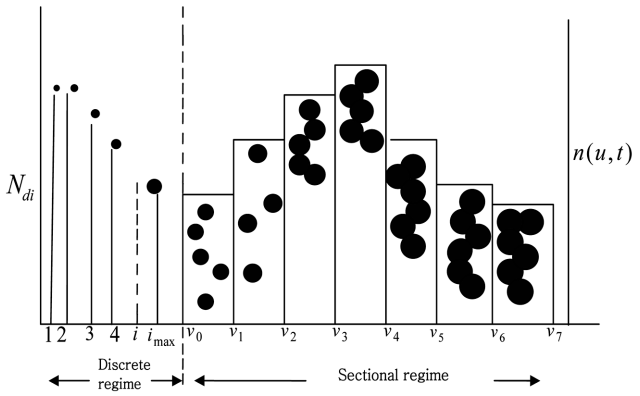

Fig. 1. Illustration of discrete and sectional regimes. N_{di} and n(u, t) represent the number of i-mers per unit volume of gas in the discrete-regime and the number distribution function for particles of volume u in the sectional regime, respectively.

†To whom correspondence should be addressed.
E-mail: kypark@kongju.ac.kr

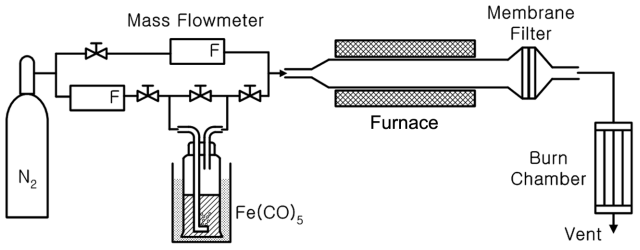

Fig. 2. Schematic drawing of experimental apparatus for thermal decomposition of $Fe(CO)_5$ vapor.

model; the particle size distribution is discretized up to a certain size past which it is represented as sectional, as shown in Fig. 1. Park and Rogak [8] developed a discrete-sectional model, in which the number of primary particles in each section, rather than the surface area, was taken as a dependent variable. Recently, we developed a discrete-sectional model [9], similar to Jeong and Choi's model in that the volume and surface area equations were used, but differ in that the surface area equations were formulated in such a way that the coagulation integrals calculated for the volume equations could be used by the area equations as well, thereby reducing computation time and memory.

This paper applies our discrete-sectional model to particle-growth analysis of iron produced by thermal decomposition of $Fe(CO)_5$ in a hot-wall reactor. Model predictions were compared with our and Giesen et al.'s [1] experimental data.

EXPERIMENTAL

The experimental setup, as shown in Fig. 2, consists of a bubbler immersed in a water bath for $Fe(CO)_5$ vaporization, a tubular furnace, and a particle collector. Nitrogen gas (99.999%) was passed at a rate of 92 ml/min, measured by a mass flow meter, to the bubbler for the gas to be loaded with $Fe(CO)_5$ vapor. Dilution nitrogen was provided to control the residence time in the reactor. The two flows were combined into one prior to the reactor. The reaction tube is made of alumina, measuring 2.4 cm in diameter and 60 cm in length, and heated by an electric heater. Produced Fe particles were collected with a Teflon membrane filter (Cole-Parmer, Model Zix 90C), the pore size of which is 0.2 μm. For the measurement of particle shape, size, and distribution, a TEM (Carl Zeiss, Model EM912 Omega) was used. From an image obtained by scanning the TEM micrograph, about 300 primary particles were selected and their sizes were determined to calculate the number average diameter by using a computer program (Image pro plus 4.0, MediaCybernetics) in which the number of pixels occupied by a particle is counted and converted into a diameter.

Operating parameter variables with the present experimental setup would be reactor set temperature, carrier gas flow rate, and precursor concentration. In the present study, however, only the reactor temperature was taken as variable and varied from 300 to 1,000 °C, holding the precursor concentration at 1.18×10^{-5} mol/L and the carrier gas rate at 30 cm^3/s. The effect of reactor temperature on particle morphology and size is our prime concern since the temperature effect on particle size has been controversial among investigators for titania particles with similar preparation methods [10].

MODELING OF PARTICLE GROWTH

In aerosol reactors, condensable product molecules are initially formed by chemical reaction. The condensable molecules then self-nucleate to form a cloud of stable nuclei that grow subsequently by collision to larger particles. The rate of change of particle numbers with respect to time and particle size can be represented by the GDE also called as the Population Balance Equation (PBE) [11] as follows:

$$\frac{\partial n}{\partial t}+\frac{\partial (Gn)}{\partial v}-I(v^*)\delta(v-v^*) = \frac{1}{2}\int_0^v \beta(v-u,u)n(v-u,t)n(u,t)du - n(v,t)\int_0^\infty \beta(v,u)n(u,t)du \quad (1)$$

The first term of the left-hand side (LHS) is the rate of change of total number of particles in the particle volume from v to v+dv. The second LHS term is the loss or gain of number of particles by condensation at a rate G. The third LHS term is the rate of formation of new particles of critical volume v^* at a rate of I. The two right-hand-side (RHS) terms are the gain and loss of particles by coagulation, respectively, in the particle volume from v to v+dv.

By applying the discrete-sectional method to the GDE, the rate of change of volume and surface area of discrete particles or particles in a section can be represented by ordinary differential equations, as shown earlier [9]. These differential equations were solved by using an ordinary differential-equation solver "ODEINT" [12], with the parameters in Tables 1 and 2 and the assumption of a product monomer as a nucleus. This assumption may be reasonable because the number of iron atoms composing a nucleus is calculated to be

Table 1. Simulation conditions for comparison with present experimental data

Reactor set temperature (°C)	300, 500, 800 and 1,000
Initial $Fe(CO)_5$ concentration at STP (mol/L)	1.18×10^{-5}
Gas flow rate at STP (cm^3/s)	30
Reaction order	1.0
Rate constant (s^{-1})	$k_r=1.93\times10^9\exp\left(-\frac{72(kJ)}{RT}\right)$ [1]
Sintering time equation	$\tau_k=0.09\frac{k_bT}{\gamma\delta^4D_{sd}}\left(\frac{3v_{pk}}{4\pi}\right)^{4/3}$ [18]
Surface diffusion coefficient	$D_{sd0}=5.2\times10^4$ cm^2/s
$D_{sd}=D_{sd0}\exp\left(\frac{E_{diff.-sd}}{RT}\right)$	$E_{diff-sd}$=221 kJ/mol [19]
Lattice spacing factor, δ(cm)	2.872×10^{-8}
Surface tension, γ(erg/cm^2)	1,000

Table 2. Simulation conditions for comparison with experimental data of Giesen et al. [1]

Reactor temperature (°C)	400 , 600 and 800
Initial reactant concentration at STP (mol/L)	1.784×10^{-4}
Reactor residence time (s)	3.17-3.95
Inside diameter of the reactor (cm)	2.2
Flow rate of gas at STP (cm^3/s)	50
Reactor length (cm)	160

smaller than 2.0 for the simulation condition in Table 1.

From the total particle volume in the k^{th} section, V_{sk}, and the particle surface area, A_{sk}, the primary particle diameter, d_{pk}, of the k^{th} section was calculated as follows:

$$d_{pk}=6V_{sk}/A_{sk} \quad (2)$$

The particle number concentration in the k^{th} section, N_{sk}, was determined by the following equation [13]:

$$N_{sk}=(V_{sk}/\Delta v_k)\ln(v_k/v_{k-1}) \quad (3)$$

The section spacing factor or the ratio of the volume range of a section to that of the section smaller by one unit, f_s, was set at 2.05. The number of discrete sizes, i_{max}, was 20. The number of discrete sizes greater than 18 was reported to be sufficient [14].

The coagulation coefficient, β, for two colliding agglomerates was used as follows [15]:

$$\beta=2\pi(d_{ci}+d_{cj})(D_i+D_j)f_D \quad (4)$$

where d_{ci} and d_{cj} are the collision diameters, D_i and D_j are the diffusion coefficients for the two agglomerates, and f_D is a correction factor to cover the entire size region from the free molecular to the continuum region [15]. The collision diameter of a spherical particle is its diameter and the collision diameter of an agglomerate composed of primary particles was determined from the equation proposed by Matsoukas and Friedlander [16], with a mass fractal dimension at 1.8.

The entire time span was divided into a number of time steps. The coagulation integrals and the sintering time were updated every time step by using the primary particle diameter at the previous time step.

RESULTS AND DISCUSSION

The reactor temperature is not constant over the entire length of the reactor. It was constant in the central zone, but decreased towards both ends. Actual temperature profile was fitted by a function in model simulation. The size range is 0.283 nm (monomer diameter) to 0.769 nm (20-mer diameter) for the discrete regime and 0.769 nm to 1 μm for the sectional regime.

1. Comparison of Model Prediction with Present Experimental Data

Fig. 3 shows the TEM images of iron particles from the thermal decomposition of $Fe(CO)_5$ vapor with the reactor temperature varying from 300 to 1,000 °C, holding the concentration of $Fe(CO)_5$ at 1.18×10^{-5} mol/L (STP) and the gas flow rate at 30 cm^3/s (STP). All the particles exhibited chain-like structures. The primary particle size increased with temperature increase up to 800 °C, and then decreased as the temperature was further increased to 1,000 °C. A similar phenomenon was observed by Nakaso et al. [17] for titania produced from either thermal decomposition of titanium tetraisopropoxide or oxidation of titanium tetrachloride in a tubular aerosol reactor at reactor temperature ranging from 800 to 1,400 °C. The primary particle size of titania showed a maximum at an intermediate temperature of about 1,200 °C.

The variation of primary particle size with reactor temperature was simulated with the present model by using the conditions in Table 1. Model prediction showed good agreement with experimental data, as shown in Fig. 4. An increase of the reactor temperature would have two opposing effects: one to increase and the other to decrease the primary particle size. The sintering rate of the primary particles within an agglomerate should increase with temperature

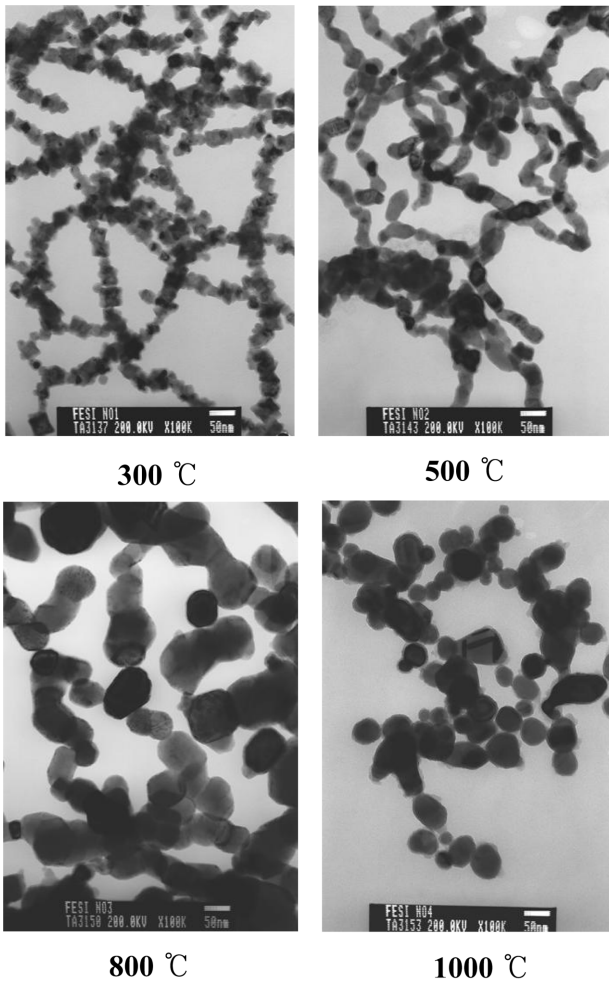

Fig. 3. TEM images of iron particles with reactor temperature varying from 300 to 1,000 °C.

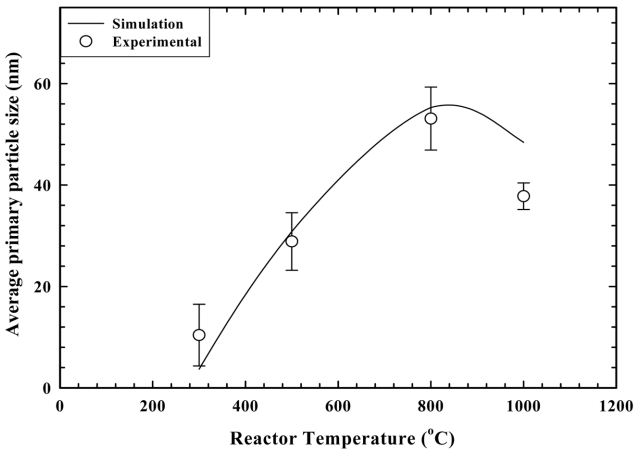

Fig. 4. Effect of reactor temperature on primary particle size with initial $Fe(CO)_5$ concentration at 1.18×10^{-5} mol/L.

to increase the size. Whereas, the time available for sintering is reduced corresponding to the decrease in reactor residence time due to gas volume expansion, and the temperature-dependent nucleation should be greater resulting in less availability of resources per nucleus for growth by condensation and surface reaction, leading to smaller primary particles. The number of primary particles composing an agglomerate or agglomerate size before a major stage of sintering between primary particles sets in may be another important factor in determining the final primary particle size. Fig. 5 shows that the number of primary particles increased initially by coagulation showed a maximum and then decreased due to a coalescence of neighboring particles by sintering. The number of particles at the maximum was higher at 800 °C by an order of magnitude than at 1,000 °C. At both temperatures, the average number of primary particles per agglomerate decreased to nearly one at the reactor exit, indicating that the primary particles had coalesced almost completely. Under such a condition of nearly full coalescence, the primary particle size must depend on the maximum number of primary particles prior to the coalescence by sintering. Thus, various effects come into play with an increase in reactor temperature. An overall effect was to decrease the primary particle size as the temperature was increased from 800 to 1,000 °C.

Fig. 6 shows the distributions of agglomerate size in volume equivalent diameter at 1, 30 and 60 cm from the reactor inlet, with the reactor temperature at 500 °C. In the early stage of particle growth or at 1 cm, a bimodal size distribution appeared because of incomplete depletion of monomers and clusters. These discrete particles were removed later by deposition on larger particles or agglomerates, making the size distribution mono-modal at the locations of 30 and 60 cm. The difference in size distribution was marginal between 30 and 60 cm, implying that the particle growth occurred primarily within the first half of the reactor length.

2. Comparison with Experimental Data by Giesen et al. [1]

Model predictions were compared with experimental data by Giesen et al. [1], with the operating conditions in Table 2 and the physical properties, the reaction rate and the sintering equation given in Table 1.

Fig. 7 shows a comparison in primary particle size between model prediction and experimental data. Considering many uncertain-

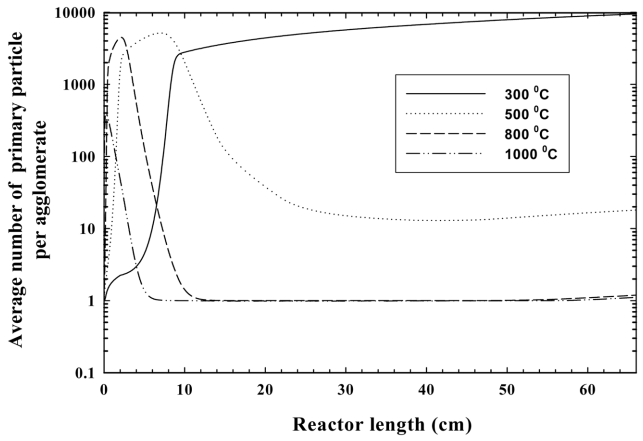

Fig. 5. Axial variation of average number of primary particles per agglomerate at four reactor temperatures, 300 , 500, 800 and 1,000 °C.

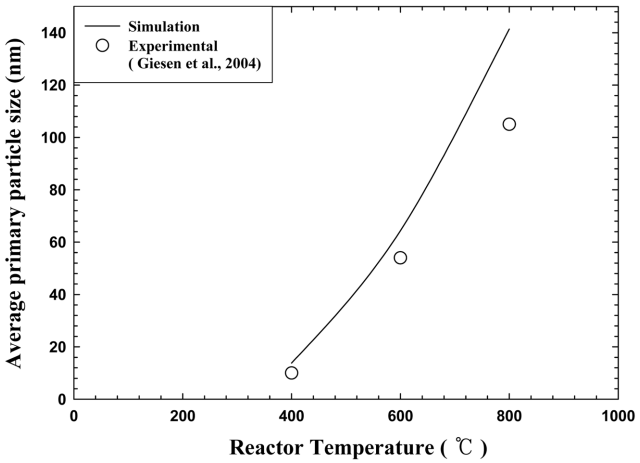

Fig. 7. Effect of reactor temperature on primary particle size with initial $Fe(CO)_5$ concentration at 1.784×10^{-4} mol/L.

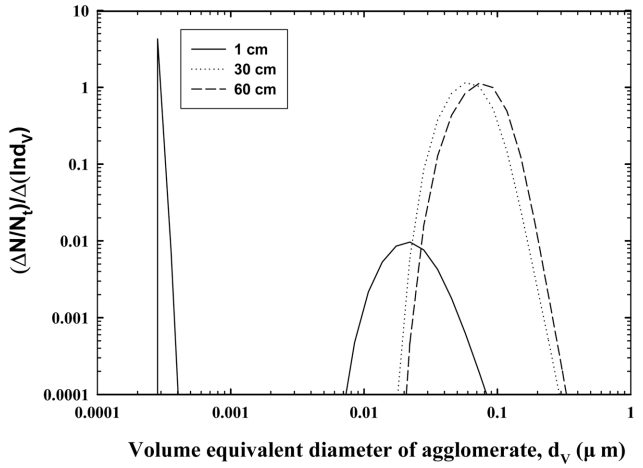

Fig. 6. Size distribution of agglomerates at 1, 30 and 60 cm from reactor inlet at a reactor temperature of 500 °C.

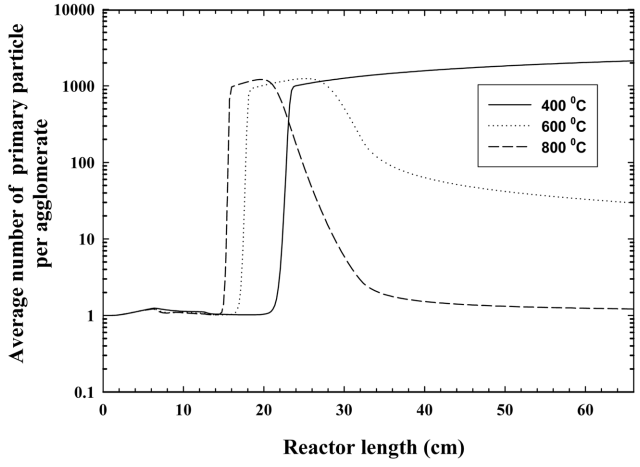

Fig. 8. Axial variation of average number of primary particles per agglomerate with varying reactor temperature.

ties involved in the model, fairly good agreement was reached. The primary particle size is more temperature-sensitive by model prediction, probably due to an over-estimation of the activation energy for sintering. The number of primary particles per agglomerate along the reactor length is shown in Fig. 8 with varying reactor set temperature. The number of primary particles per agglomerate at the reactor outlet was about 1,000 and 100, respectively, at 400 and 600 °C. The number decreased to nearly one at 800 °C, implying that the particles exiting the reactor at that temperature are nearly spherical, not in agglomerated form.

The primary-particle size distributions were compared between model prediction and experimental data at three reactor temperatures, 400, 600, and 800 °C. The results are shown in Figs. 9, 10 and 11, respectively. In these figures, the normalized number fraction is defined by the particle number in a size segment divided by the largest particle number among size segments. At 400 °C, the distribution was narrower by model prediction, the peak appearing at the right end, as shown in Fig. 9. A similar distribution was reported for titania by Tsantilis and Pratsinis [6]. The size corresponding to the peak may be the maximum size attainable by sintering at that temperature. The smaller primary particles are expected to eventually grow to the maximum size provided with a longer residence time in the reactor, yielding a mono-dispersed distribution.

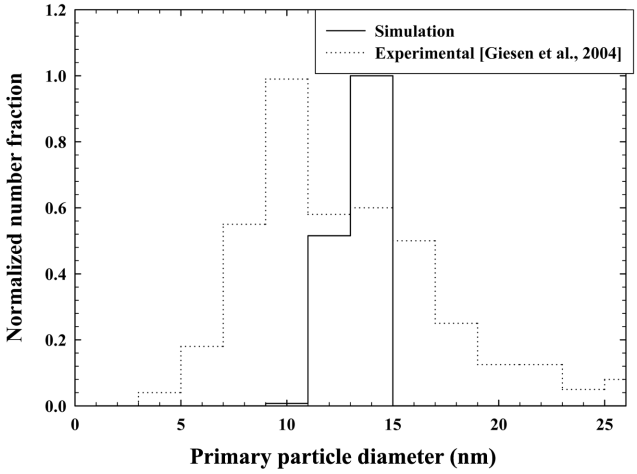

Fig. 9. Comparison between simulation and experimental data of primary particle size distribution at a reactor temperature of 400 °C.

At a higher temperature of 600 °C the sintering appears to have proceeded so sufficiently in all agglomerates that mono-dispersity could be attained, as shown in Fig. 10. The primary-particle size distributions predicted by the present model deviate considerably from experimental observations. The assumption used in the model that the primary particle size is uniform within a section may be a reason for the deviation. Another reason may be in the residence time distribution. In the model, a uniform residence time distribution was assumed, while in the experiments the distribution was probably not uniform by examining the geometry of the reactor and the experimental conditions including the gas flow rate.

As the temperature was increased to 800 °C, the size distribution predicted by model broadened remarkably, as shown in Fig. 11. It turned even broader than experimental data. At this temperature, all the particles in an agglomerate have been nearly coalesced into a spherical particle, as shown in Fig. 8. In this situation, the particle size is determined by the agglomerate size before the coalescence of the primary particles, which is distributed broadly. The particle size, therefore, should exhibit a broad distribution.

CONCULSION

The growth of iron particles by thermal decomposition of $Fe(CO)_5$ in a tubular reactor was analyzed by using a one dimensional discrete-sectional model, taking into account the coalescence by sintering of neighboring particles within agglomerate. A unique feature of the model is that most of the integrals calculated for the volume equations could be used for the surface area equations as well, thereby reducing computational load. Model predictions were compared with two sets of experimental data, showing good agreement with experimental data in primary particle size, but a considerable devi-

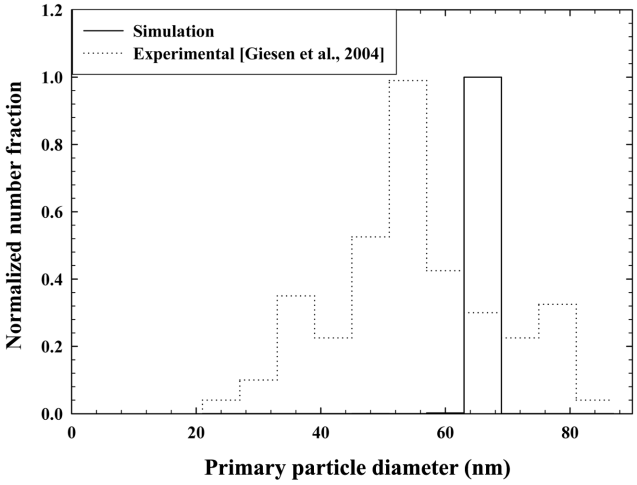

Fig. 10. Comparison between simulation and experimental data of primary particle size distribution at a reactor temperature of 600 °C.

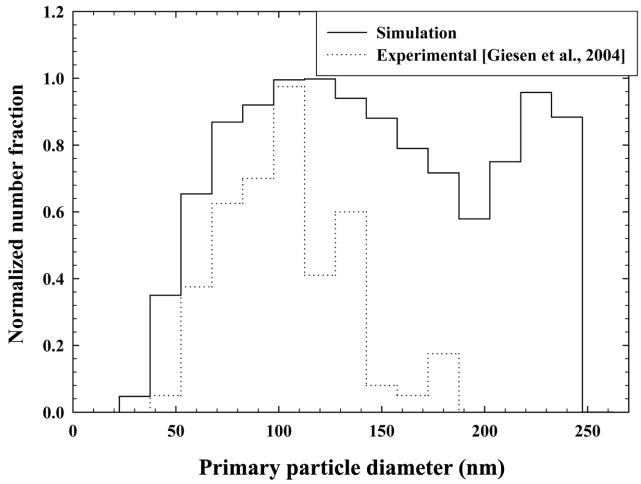

Fig. 11. Comparison between simulation and experimental data of primary particle size distribution at a reactor temperature of 800 °C.

ation in primary particle size distribution. The deviation may be due to an inadequate understanding of the sintering mechanism for the particles within an agglomerate, and to the assumption of ideal plug flow in the reactor in contrast to the non-ideal dispersive flow in an actual reactor.

ACKNOWLEDGMENT

This work was supported by grant No. (R01-2002-000-004-0) from Korea Science & Engineering Foundation.

NOMENCLATURE

A_{si} : total surface area of particles in the i^{th} section per unit volume of gas [cm^2 cm^{-3}]
D_i : diffusion coefficient for the agglomerates in the i^{th} section [cm^2 s^{-1}]
d_{ci} : collision diameters of agglomerates in the i^{th} section [cm]
d_{pi} : primary-particle diameter in the i^{th} section [cm]
d_v : volume equivalent diameter of agglomerate [μm]
D_{sd} : diffusion coefficient for surface diffusion [cm^2 s^{-1}]
D_{sd0} : pre-exponential factor of the surface-diffusion equation in Table 1 [cm^2 s^{-1}]
$E_{diff,sd}$: activation energy for surface diffusion in Table 1 [kJ mol^{-1}]
f_D : correction factor to cover both free-molecular and continuum regime
f_s : section spacing factor
G : particle growth rate by condensation [cm^3 s^{-1}]
I : nucleation rate of product monomer [molecules cm^{-3}]
i_{max} : maximum number of nuclei composing a discrete particle
k_b : Boltzmann constant [erg $molecule^{-1}$ K^{-1}]
k_r : reaction rate constant [s^{-1}]
n(u, t) n(v, t) : size distribution function for particle volume u and v, respectively [cm^{-6}]
N_{di} : total number of i-mers per unit volume of gas [cm^{-3}]
N_{sk} : total number of particles in the k^{th} section per unit volume of gas [cm^{-3}]
t : time [s]
T : temperature [K]
u, v : agglomerate or particle volume [cm^3]
v_m : monomer volume [cm^3]
v^* : critical volume in Eq. (1) [cm^3]
v_{k-1} : lower limit of the particle volume of the k^{th} section [cm^3]
v_k : upper limit of the particle volume of the k^{th} section [cm^3]
Δv_k : volume interval of the k^{th} section [cm^3]
V_{sk} : total particle volume in the k^{th} section per unit volume of gas [cm^3 cm^{-3}]

Greek Letters

β(u, v) : collision coefficient for two particles of volume u and v [cm^3 s^{-1}]
τ_k : characteristic coalescence time in the k^{th} section [s]
δ : lattice parameter [cm]
γ : surface tension [erg cm^{-1}]

REFERENCES

1. B. Giesen, H. R. Orthner, A. Kowalik and P. Roth, *Chem. Eng. Sci.*, **59**, 2201 (2004).
2. H. Hofmeister, F. Huisken, B. Kohn, R. Alexandrescu, S. Cojocaru, A. Crunteanu, I. Morjan and L. Diamandescu, *Appl. Phys. A.*, **72**, 7 (2001).
3. K. Y. Park, J. K. Park and S. H. Lim, *J. Mater. Res.*, **18**, 2285 (2003).
4. C. J. Choi, B. K. Kim, O. Tolochko and L. Da, *Rev. Adv. Mater. Sci.*, **5**, 487 (2003).
5. Y. Xiong and S. E. Pratsinis, *J. Aerosol Sci.*, **24**, 283 (1993).
6. S. Tsantilis and S. E. Pratsinis, *AIChE J.*, **46**, 407 (2000).
7. J. I. Jeong and M. Choi, *J. Aerosol Sci.*, **32**, 567 (2001).
8. S. H. Park and S. N. Rogak, *Aerosol Sci. Technol.*, **37**, 947 (2003).
9. C. G. Moniruzzaman and K. Y. Park, *Korean J. Chem. Eng.*, **23**, 159 (2006).
10. K. Y. Park, M. Ullmann, Y. J. Suh and S. K. Friedlander, *J. Nanoparticle Res.*, **3**, 309 (2001).
11. S. K. Friedlander, *Smoke, dust and haze*, Wiley, New York (1977).
12. W. H. Press, S. A. Teukolsky, W. T. Vetterling and B. P. Flannery, *Numerical recipes in FORTRAN 77*, Cambridge University Press (1992).
13. J. D. Landgrebe and S. E. Pratsinis, *J. Colloid Interface Sci.*, **139**, 63 (1990).
14. J. J. Wu and R. C. Flagan, *J. Colloid Interface Sci.*, **123**, 339 (1988).
15. S. N. Rogak and R. C. Flagan, *J. Colloid Interface Sci.*, **151**, 203 (1992).
16. T. Matsoukas and S. K. Friedlander, *J. Colloid Interface Sci.*, **146**, 495 (1991).
17. K. Nakaso, T. Fujimoto, T. Seto, M. Shimada, K. Okuyama and M. M. Lunden, *Aerosol Sci. Technol.*, **35**, 929 (2001).
18. P. C. Knight, J. Seville, H. Kamiya and M. Horio, *Chem. Eng. Sci.*, **55**, 4783 (2000).
19. G. Matsumura, *Acta Metall.*, **19**, 851 (1971).